Carbohydrate Polymers 86 (2011) 1048–1054

Contents lists available at ScienceDirect

Carbohydrate Polymers

journal homepage: www.elsevier.com/locate/carbpol

Incorporation of protein-loaded microspheres into chitosan-polycaprolactone scaffolds for controlled release

Jiliang Wu [a], Chunyan Liao [b], Jun Zhang [c], Wenze Cheng [b], Nuo Zhou [d,*], Sheng Wang [b], Ying Wan [b,**]

[a] The Cardiovascular, Cerebrovascular, and Metabolic Disorder Research Institute, Xianning University, Xianning 437100, PR China
[b] College of Life Science and Technology, Huazhong University of Science and Technology, Wuhan 430074, PR China
[c] Department of Chemistry and Chemical Engineering, Royal Military College of Canada, Kingston, Ontario, Canada K7K 7B4
[d] The Affiliated Stomatology Hospital, Guangxi Medical University, Nanning 530021, PR China

ARTICLE INFO

Article history:
Received 5 May 2011
Received in revised form 26 May 2011
Accepted 26 May 2011
Available online 6 June 2011

Keywords:
Chitosan microsphere
Transforming growth factor
Controlled release
Scaffold
Compressive property

ABSTRACT

Chitosan microspheres loaded with transforming growth factor-β1 (TGF-β1) were first prepared with an emulsification method using genipin as crosslinker, and the selected microspheres were then embedded into porous scaffolds built by chitosan-polycaprolactone with polycaprolactone content of around 42 wt.%. Some optimized chitosan-polycaprolactone scaffolds with porosity higher than 80% and having an initial TGF-β1 load of around 3 ng(TGF-β1)/mg(dry scaffold) were capable of maintaining sustained release of TGF-β1 in a simulant *in vivo* environment at controlled rates over a period of time longer than four weeks without severely initial burst. The chitosan-polycaprolactone scaffolds also showed well-defined compressive properties in wet state with compressive stress at 10% strain and modulus higher than 100 kPa and 1000 kPa, respectively, which are almost ten-fold higher than that of corresponding microsphere-embedded chitosan scaffolds. The obtained results suggest that potential applications of the scaffolds in articular cartilage repair.

1. Introduction

Lesions to articular cartilage occur very often due to sport injuries and other joint traumas. Natural repair of articular cartilage is very limited since articular cartilage has an extended extracellular matrix with very few cells and is lack of blood supply (Chiang and Jiang, 2009; Pearle, Warren & Rodeo, 2005). Although articular cartilage lesions involved with small lateral extent and confined to the partial thickness could be healed by filling with a matrix containing appropriate proteins and drugs at requisite concentrations (Sterodimas, Faria, Correa & Pitanguy, 2009), repair of the articular cartilage with larger lateral extent and full thickness still remains a major challenge in clinic practices (Haleem and Chu, 2010; Muzzarelli, 2009a).

Many studies on articular cartilage have suggested that some growth factors can significantly improve the repair of articular cartilage with the aid of suitable scaffolds (Rutgersy, Pelty, Dhertyz, Creemersy & Saris, 2010). Of various growth factors, transforming growth factor-β1(TGF-β1) has been considered to be a favorable one because of its functions in the growth and differentiation of various cells. It has been reported that TGF-β1 can recruit some kinds of cells, such as chondroblasts and bone marrow stromal cells, from the synovial membrane, perichondrium and periosteum, and promote them to differentiate into chondrocytes (Hunziker, 2001). Nevertheless, *in vivo* administration of ectogenic TGF-β1 is frequently limited because TGF-β1 is short-lived if it is exposed to a physiological environment (Whitaker, Quirk, Howdle & Shakesheff, 2001). To protect TGF-β1 from proteolysis and antibody neutralization and to maintain its activity *in vivo* for the required period of time, proper carriers for delivery of TGF-β1 are normally required (Hoshiba et al., 2011; Shalaby, 1994).

In the cases of protein delivery by means of scaffolds, directly incorporating proteins into designated scaffolds seems to be feasible since the resulting scaffolds could possibly function as protein-carriers while supporting the growth of seeded cells. However, there are several concerns about this kind of method (Puppi, Chiellini, Piras & Chiellini, 2010; Muzzarelli, 2011): (1) excess amount of protein is usually needed to reach a therapeutic level due to the large volume of the scaffolds; (2) administration of release dose of proteins becomes difficult because the scaffolds usually have large pore sizes and high porosity, resulting in significant initial burst; and (3) uncertain protein compatibility stemmed from scaffolds may attenuate or even inactivate the bioactivity of proteins since the main

* Corresponding author.
** Corresponding author. Tel.: +86 27 87792216; fax: +86 27 87792205.
E-mail addresses: nuozhou@hotmail.com (N. Zhou), ying_x_wan@yahoo.ca (Y. Wan).

0144-8617/$ – see front matter © 2011 Elsevier Ltd. All rights reserved.
doi:10.1016/j.carbpol.2011.05.060

requirements for the scaffolds are focused on their biocompatibility, mechanical properties and biodegradable characteristics in stead of their ability for maintaining the bioactivity of proteins. To achieve sustained and controlled release of TGF-β1 from desirable scaffolds while maintaining the bioactivity of TGF-β1, in the present study, TGF-β1 was first loaded into chitosan microspheres crosslinked by genipin, and the resulting microspheres were then incorporated into porous chitosan-polycaprolactone (chitosan-PCL) scaffolds. It is expected that TGF-β1 could be controllably released from these scaffolds over a longer period of time without significant burst whereas the scaffolds have desired compressive strength in wet state.

2. Experimental

2.1. Materials

Chitosan with medium molecular weight was received from Aladdin Inc. To obtain highly deacetylated chitosan, the received samples were deacetylated in a 50 wt.% NaOH solution for 2 h at 100 °C, and the alkali treatment was repeated once. Degree of deacetylation of resulting chitosan was measured as 92.7(±1.8)%, following a reported method (Wan, Creber, Peppley & Bui, 2003). The human recombinant TGF-β1 was supplied by PeproTech Inc. Lysozyme, genipin and caprolactone were purchased from Sigma–Aldrich. All other chemicals were obtained from normal commercial channels in China and they all were of analytical grade.

2.2. Preparation of TGF-β1-loaded chitosan microspheres

TGF-β1-loaded microspheres were prepared with an emulsification method using genipin as crosslinker. Chitosan was dissolved in 1.0% aqueous acetic acid solution to produce 2 wt.% solutions. To each solution, a known amount of TGF-β1 dissolved in 4 mM HCl was introduced and the mixtures were emulsified with n-octanol containing 4 wt.% Span-80 under homogenization at 3000 rpm for 20 min. Afterwards, various amounts of aqueous genipin solution (2.5 wt.%) were dropwise added into the emulsions during stirring, and the mixtures were homogenized at 37 °C for additional 1.0 h. The microspheres were collected by centrifugation, repeatedly washed with isopropyl alcohol and distilled water, and lyophilized at −75 °C in a freeze-drier.

2.3. Fabrication of microsphere-embedded chitosan-PCL scaffolds

Chitosan-PCLs were synthesized using reported methods (Liu, Chen & Fang, 2006; Wu et al., 2011). Some chitosan-PCLs with PCL weight percentage of 42.8(±1.62) wt.% were selected for fabrication of scaffolds. In a typical experiment, the employed chitosan-PCL was dissolved in 1.0% aqueous acetic acid solution to produce 2.0 wt.% chitosan-PCL solutions. To each solution, a known amount of microspheres was added, and the resulting mixtures were thoroughly homogenized at 37 °C and concentrated into gel-like fluids under reduced pressure using a chamber equipped with a regular air pump. The mixtures were then cast onto Teflon dishes, frozen at −20 °C for a required duration and lyophilized at −75 °C. The resulting microsphere-embedded chitosan-PCL scaffolds were neutralized in NaOH–CH_3CH_2OH aqueous solution (NaOH was dissolved in 60% ethanol aqueous solution with a 0.5 wt.% concentration), washed with distilled water until neutral pH and lyophilized again prior to further characterization. Some microsphere-embedded chitosan scaffolds were also prepared with the same protocol and used as controls.

2.4. Characterization

The content of C, H, and N in chitosan-PCLs was measured using an elemental analyzer and the weight percents of PCL in chitosan-PCLs were calculated on the basis of elemental analysis.

The sizes and shapes of microspheres were viewed under a scanning electron microscope and the average size was determined using a computed image analysis system by measuring the diameters of 100 microspheres at 100 different lattices in a SEM image for each specimen.

Porosity of scaffolds was calculated as follows (Wan, Wu, Xiao, Cao & Dalai, 2009):

$$\text{Porosity} = \frac{V - (W/\rho)}{V} \times 100\% \quad (1)$$

where V is the volume of scaffold (cm^3), W is the mass of scaffold (g), ρ is the density of nonporous film (g/cm^3), and it was determined with a floating method using mixed solvents composed of carbon tetrachloride (density: 1.586 g/cm^3) and ethanol (density: 0.816 g/cm^3).

The average pore-size of scaffolds was estimated by measuring 100 different pores in a SEM image for each scaffold using the computed image analyzer mentioned above.

2.5. Loading efficiency of microspheres

Loading efficiency of microspheres was determined by using an extraction method. Microspheres were cryogenically ground into powder. A precisely weighed quantity of powder was extracted with 4 mM HCl solution at 37 °C for 2 h using a water bath shaking at 100 rpm. The extraction of the same powder was repeated three times and supernatants were collected by centrifugation. The accumulated supernatants were assayed for TGF-β1 concentrations using TGF-β1 ELISA Kit (eBioscience Inc., USA), as directed by the manufacturer. Optical density was measured using a microplate reader at 450 nm. Loading efficiency was calculated as follows:

$$\text{Loading efficiency} = \frac{W_{\text{initial}}}{W_{\text{feed}}} \times 100\% \quad (2)$$

where W_{initial} is the measured weight of TGF-β1 in microspheres, and W_{feed}, the fed weight of TGF-β1 during microsphere preparation (ng (TGF-β1)/mg (dry chitosan powder)).

2.6. Swelling index

Swelling index of microspheres or scaffolds in lysozyme bearing PBS (lysozyme: 10^4 U/mL) media was measured via a gravimetric method. Weighed dry microspheres or scaffolds (weight: W_d) were immersed in lysozyme bearing PBS solutions at ambient temperature until swelling equilibrium was attained. Wet samples were then transferred into some thimbles and excess water was removed by centrifugation at 2000 rpm for 1 min prior to measuring their weight (W_w). Swelling index was calculated as follows:

$$\text{Swelling index} = \frac{W_w - W_d}{W_d} \times 100\% \quad (3)$$

2.7. Measurements of compressive mechanical parameters

Compressive parameters of scaffolds in wet state were measured using an Instron universal testing machine at ambient temperature. The dry scaffolds were cut into circular pieces with a dimension of 10 mm in diameter and around 5 mm in thickness, and immersed in PBS solution for 2 h prior to measurements. After removal of excess water by centrifugation, these pieces were compressed at a crosshead speed of 1 mm/min. The compressive

modulus (E) was defined as the initial linear modulus and the stress at 10% strain was recorded as σ_{10}.

2.8. In vitro release of TGF-β1

TGF-β1 releases from microspheres or scaffolds were examined using lysozyme bearing PBS media (lysozyme: 10^4 U/mL). In the cases of microspheres, carefully weighed amounts of microspheres were introduced into glass vials with a known volume of buffer containing 0.02% sodium azide as the preservative. These vials were vortexed on a shaker table at 37 °C, 60 rpm. The supernatants were retrieved at each time point, and meanwhile, each vial was replaced with the same volume of fresh buffer. The amount of TGF-β1 was determined using TGF-β1 ELISA Kit mentioned earlier. The released amount of TGF-β1 was calculated by correlating to a standard curve. In the cases of microsphere-embedded scaffolds, the same protocol was used.

2.9. Statistical analysis

Analysis of variance was performed using statistical software (SPSS 15.0 for Windows) to determine whether there were significant differences among the measured data. The threshold for statistical significance was set at $p < 0.05$.

3. Results and discussion

3.1. Morphology and parameters of TGF-β1-loaded chitosan microspheres

The natural crosslinker, genipin, was selected for the preparation of microspheres in consideration of its low cytotoxicity. For example, genipin is about 5000–10,000 times less cytotoxic than commonly used glutaraldehyde (Muzzarelli, 2009b; Yuan et al., 2007). Fig. 1(A) presents a representative SEM image for TGF-β1-loaded chitosan microspheres. Morphology of these microspheres showed good sphericity and had smooth surface without cracks or wrinkles, and they had various sizes changing from around 2 to about 40 μm. To examine the effect of crosslinker on the average sizes, loading efficiency and swelling index of microspheres, several sets of microspheres were fabricated using various amounts of genipin under the same processing conditions, and relevant parameters for them are provided in Table 1.

Data in Table 1 point out that average size and swelling index of microspheres showed significant decreasing trends until the feed ratio of genipin to chitosan reached around 1:8 mg/mg ($p < 0.05$), and after that, microspheres only had small changes in their average size and swelling index; on the other hand, loading efficiency of microspheres exhibited a reverse trend, revealing these parameters can be effectively regulated by controlling the amount of genipin, and they would not substantially further change under the present processing conditions even though an increasing feed ratio higher than 1:8 was applied. The maximum feed ratio of genipin to chitosan was thus selected as 1:4 mg/mg. In addition, in considering that loading efficiency of chitosan-A and chitosan-B microspheres was very low, only four sets of microspheres, namely, chitosan-C, chitosan-D, chitosan-E and chitosan-F, were selected for further investigations.

It was noted that several main processing parameters could markedly influence the initial loading of TGF-β1 in microspheres and hence, processing parameters were carefully optimized by mainly changing the fed amount of TGF-β1 and washing times to ensure the initial TGF-β1 loading for these microspheres to be around 30 ng(TGF-β1)/mg(dry microsphere) so that the effect of the initial TGF-β1 load on the release properties of microspheres could be greatly reduced.

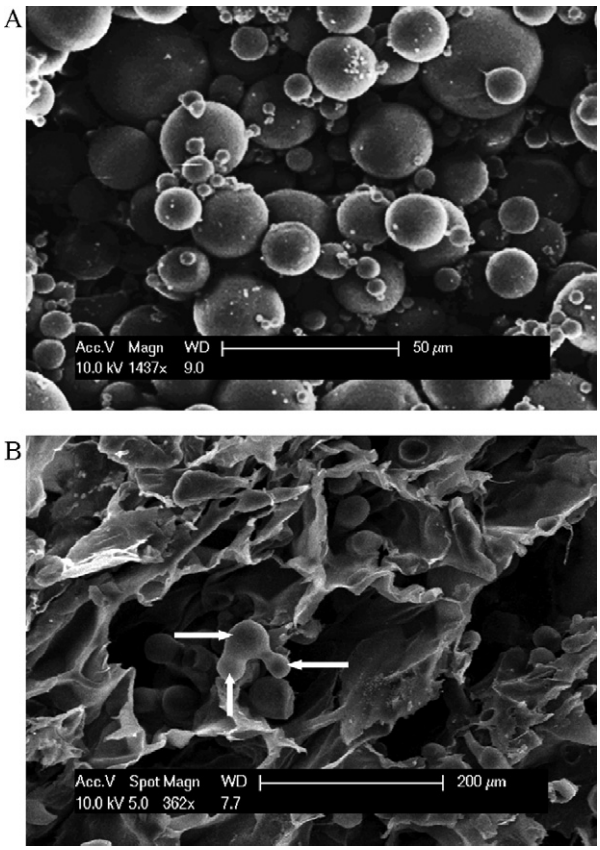

Fig. 1. SEM micrographs of (A) TGF-β1-loaded chitosan microspheres prepared under optimized processing conditions (feed ratio of genipin to chitosan was 1:6 mg/mg) and (B) microsphere-embedded chitosan-PCL scaffold (PCL content in chitosan-PCL: around 42 wt.%).

3.2. Morphology and parameters of microsphere-embedded chitosan-PCL scaffolds

TGF-β1-loaded chitosan microspheres had a quite wide size-distribution, as indicated in Fig. 1(A), and meantime, data for the average size in Table 1 also showed large differences among different sets of microspheres. To diminish the effect of microsphere-size on the release profiles of TGF-β1, each set of microspheres was sieved into three groups using sifters with mesh sizes of 325 and 500, and the corresponding size for three groups of microspheres in each set was less than 25 μm, between 25 and 45 μm and larger than 45 μm in order. Only those microspheres with sizes between 25 and 45 μm in each set were selected for the scaffold fabrication.

Fig. 1(B) shows a typical image of the chitosan-PCL scaffold. It can be observed that the scaffold has interconnected pores in irregular shapes, and TGF-β1-loaded chitosan microspheres were randomly dispersed into the scaffold. The microspheres were either mounted onto or just simply laid down the wall of pores, and some of them already lost their originally well-defined sphericity due to the coating effect arisen from chitosan-PCL, which is evidenced by those agglutinated microspheres indicated by the white arrows in Fig. 1(B).

Four sets of chitosan-PCL scaffolds with similar porosities and average pore sizes were fabricated using chitosan-C, chitosan-D, chitosan-E and chitosan-F microspheres in order to examine the effect of microspheres on release profiles of the scaffolds, and relevant parameters for the scaffolds are summarized in Table 2.

Table 1
Parameters of TGF-β1-loaded chitosan microspheres.

Samples	Feed ratio of genipin to chitosan (mg/mg)	Average size (μm)	Swelling index (%)	Loading efficiency (%)
Chitosan-A	1:15	74.7(±7.2)	117.4(±6.7)	50.1(±5.6)
Chitosan-B	1:12	55.4(±5.3)	98.3(±5.9)	61.7(±3.8)
Chitosan-C	1:10	42.1(±4.1)	86.5(±4.8)	70.2(±2.6)
Chitosan-D	1:8	32.2(±2.4)	77.2(±3.5)	76.9(±2.8)
Chitosan-E	1:6	27.3(±2.1)	72.4(±3.3)	80.8(±2.4)
Chitosan-F	1:4	23.6(±1.9)	68.3(±3.1)	83.1(±2.7)

Table 2
Parameters of chitosan-PCL and chitosan scaffolds embedded with different kinds of microspheres.[a]

Samples[b,c]	Porosity (%)	Average pore 'size (μm)	Swelling index (%)	E (kPa)[d]	σ_{10} (kPa)[e]
Chitosan-PCL(I)	91.7(±3.1)	152.5(±12.9)	44.1(±3.3)	1408.1(±121.6)	128.2(±14.5)
Chitosan-PCL(II)	90.3(±3.4)	142.7(±13.2)	43.5(±3.1)	1297.6(±116.2)	132.6(±15.2)
Chitosan-PCL(III)	91.2(±3.2)	146.1(±12.7)	46.2(±3.2)	1329.7(±109.8)	140.3(±17.9)
Chitosan-PCL(IV)	89.6(±2.9)	155.8(±14.1)	42.8(±2.6)	1386.5(±113.5)	139.6(±14.1)
Chitosan-(I)	90.9(±3.3)	143.6(±15.3)	70.6(±3.7)	137.1(±37.8)	13.4(±2.3)
Chitosan-(II)	88.6(±3.2)	149.2(±12.4)	71.1(±3.4)	123.8(±31.6)	12.9(±3.1)
Chitosan-(III)	92.2(±3.5)	154.3(±14.8)	73.5(±3.5)	135.6(±36.3)	14.3(±2.9)
Chitosan-(IV)	91.4(±3.1)	157.2(±12.5)	72.9(±3.8)	126.1(±32.1)	13.1(±2.7)

[a] Initial TGF-β1 load in these scaffolds was controlled as around 3 ng (TGF-β1)/mg (dry scaffold) by changing the amount of added microspheres.
[b] Chitosan-PCL(i) (i = I, II, III and IV) denotes scaffolds fabricated by using chitosan-PCL as matrix and chitosan-C, chitosan-D, chitosan-E and chitosan-F as embedded microspheres, respectively;
[c] Chitosan (j) (j = I, II, III and IV) refers to scaffolds built by using chitosan as matrix and chitosan-C, chitosan-D, chitosan-E and chitosan-F as embedded microspheres, respectively.
[d] E was measured for hydrated scaffolds.
[e] σ_{10} was measured for hydrated scaffolds.

Some reports have revealed that a dose of around 2 ng(TGF-β1)/mg(composite) or slightly higher is therapeutically effective for the treatment of full and partial thickness rabbit and porcine articular cartilage defects (Giannoni and Hunziker, 2003; Hunziker, 2001). In the present instance, the scaffolds were thus endowed with an initial load of TGF-β1 at around 3 ng(TGF-β1)/mg(dry scaffold) by using different amounts of microspheres. In addition, three sets of chitosan-PCL scaffolds with various porosities and average pore-sizes were also built by using chitosan-E as embedded microspheres to investigate the impact of pore parameters on the properties of scaffolds, and the relevant parameters are listed in Table 3.

Data in Table 2 indicate that there were no substantial differences ($p > 0.05$) in the pore parameters for chitosan-PCL scaffolds or for chitosan scaffolds despite the fact that swelling index of chitosan-PCL scaffolds was much lower than that of matched chitosan scaffolds. The notably lower swelling index of chitosan-PCL scaffolds can be ascribed to the hydrophobic PCL component in chitosan-PCL (Wan et al., 2009). In the cases of scaffolds listed in Table 3, it can be seen that pore parameters imposed a significant impact on swelling index of scaffolds. These results are reasonable if more details are figured out. As described in Section 2, chitosan-PCL scaffolds were built by using a 1.0% aqueous acetic acid solution. In considering that chitosan-PCLs consisted of hydrophilic chitosan main chains and hydrophobic PCL side chains, it is rational to believe that PCL side chains could turn inward and tangle together to some extent while chitosan main chains would stretch outward and enwrap those hydrophobic PCL domains during the preparation of chitosan-PCL scaffolds, as a result, the chitosan-PCL scaffolds having bigger pore-size and higher porosity would provide a larger hydrophilic surface area when exposed to aqueous media, concomitantly resulting in their higher swelling index, as manifested in Table 3.

3.3. Compressive properties of microsphere-embedded chitosan-PCL scaffolds

The compressive mechanical properties of porous scaffolds in the wet state are of particular importance in articular cartilage repair since they are very closely linked to the durability and dimension-maintaining ability of the scaffolds in practical operations and applications (Hutmacher, 2000; Shalaby, 1994). It can be seen from Table 2 that (1) there were no significant differences ($p > 0.05$) in E and σ_{10} for chitosan-PCL scaffolds, and a similar result was also recorded for chitosan scaffolds even though various amounts of microspheres were applied to these scaffolds; and (2) the E and σ_{10} of chitosan-PCL scaffolds were almost ten-fold higher than that of chitosan scaffolds. The insignificant effect from different microspheres may be attributed to the lower percentage of microspheres in the scaffolds since chitosan microspheres con-

Table 3
Parameters of chitosan-PCL scaffolds embedded with the same kind of microspheres.[a,b]

Samples[c]	Porosity (%)	Average pore size (μm)	Swelling index (%)	E (kPa)[d]	σ_{10} (kPa)[e]
Chitosan-PCL(a)	95.6(±3.9)	171.4(±16.7)	52.2(±3.4)	1082.7(±94.2)	107.1(±11.3)
Chitosan-PCL(b)	87.4(±3.1)	154.9(±12.1)	44.7(±3.1)	1346.5(±107.9)	143.2(±12.1)
Chitosan-PCL(c)	80.3(±3.4)	139.1(±14.6)	37.5(±2.7)	1672.3(±164.6)	176.4(±16.5)

[a] Initial TGF-β1 load in the scaffolds was selected as around 3 ng (TGF-β1)/mg (dry scaffold).
[b] Pore parameters were controlled by mainly changing the concentrations of CH-PCL solutions and freeze temperatures.
[c] Chitosan-PCL(k) (k = a, b and c) denotes scaffolds fabricated by using chitosan-PCL as matrix and chitosan-E as embedded microspheres.
[d] E was measured for hydrated scaffolds.
[e] σ_{10} was measured for hydrated scaffolds.

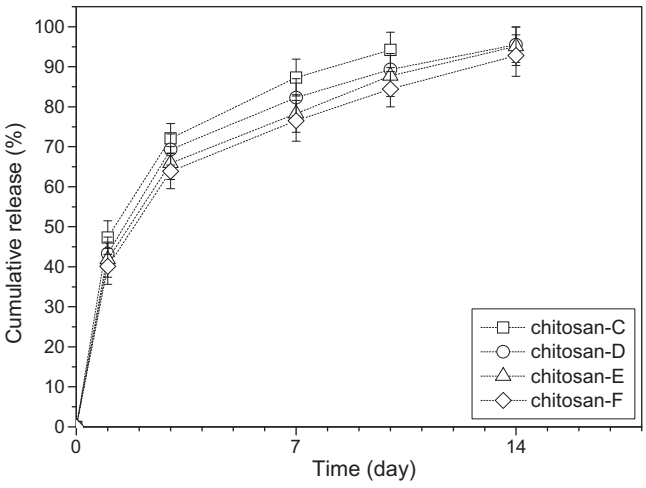

Fig. 2. Release profiles of TGF-β1-loaded chitosan microspheres.

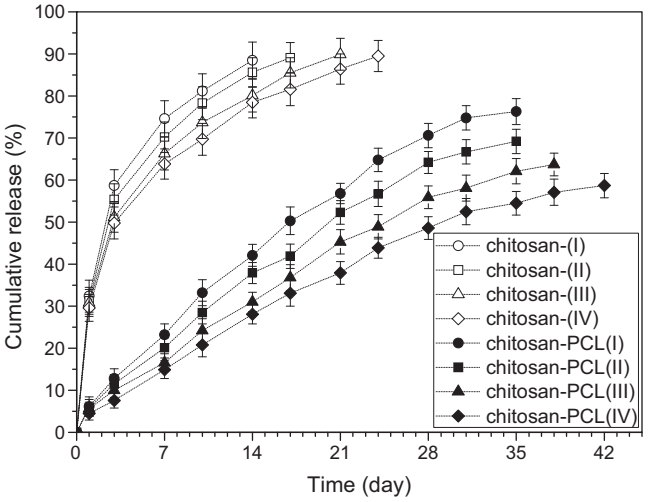

Fig. 3. Release profiles of microsphere-embedded scaffolds with similar pore parameters.

tained their initial TGF-β1 load of around 30 ng(TGF-β1)/mg(dry microsphere) whereas chitosan-PCL or chitosan scaffolds were only endued with TGF-β1 content of about 3 ng(TGF-β1)/mg(dry scaffold). In comparison with chitosan scaffolds, the high E and σ_{10} of chitosan-PCL scaffolds should be assigned to the function derived from PCL component. Many hydrophobic PCL domains formed during fabrication of the scaffolds in aqueous media would reside inside the scaffolds and act as physically crosslinked sites, which is somewhat similar to the cases of chitosan-polylactide gels described elsewhere (Qu, Wirsen & Albertsson, 1999), resulting in remarkably enhanced compressive strength in wet state.

Data in Table 3 reveal that the E and σ_{10} of chitosan-PCL scaffolds could also be regulated by the pore parameters and they significantly increased as the porosity and average pore-size decreased ($p < 0.05$). In particular, chitosan-PCL(a) scaffolds with the porosity of about 95% were still able to maintain their E and σ_{10} at around 1000 kPa and 100 kPa in the wet state, respectively, suggesting that these scaffolds are strong enough for *in vivo* applications in articular cartilage repair (Chung and Burdick, 2008).

3.4. *In vitro* release of TGF-β1

3.4.1. *Release profiles of TGF-β1-loaded chitosan microspheres*

The measurements for TGF-β1 releases were carried out in the lysozyme bearing PBS system which functions as a simulant *in vivo* environment (Ozbas-Turan, Akbuga & Aral, 2002) since these microspheres will be potentially used *in vivo*. The release profiles of TGF-β1 from different microspheres as function of time are shown in Fig. 2. The microspheres released around 40% of initially loaded TGF-β1 during the first day and after that, more than 70% of TGF-β1 was released within the first week, and the total accumulative amount of TGF-β1 was higher than 80% for all microspheres after two-week release. As described in Section 2, TGF-β1-loaded chitosan microspheres were built via an interface-crosslinking pathway through dispersed aqueous phases and a continuous octanol phase. It is reasonable to believe that only the surface or superficial layers of microspheres had been crosslinked to a certain extent and the internal layers and interior of the microspheres are freed from crosslinking, and consequently, TGF-β1 in microspheres was only physically entangled chitosan chains during the fabrication of the microspheres. Once exposed to aqueous media, the microspheres were swollen to some extent and the physical entanglement between chitosan chains and TGF-β1 molecules would be easily disentangled because of the hydrophilicity of both chitosan and TGF-β1, leading to significantly initial burst and followed fast release of entrapped TGF-β1. In addition, although these microspheres were already crosslinked by using various amounts of genipin (see Table 1) they showed quite similar the release behavior with small differences in their release patterns ($p > 0.05$), meaning that the amount of crosslinker can not effectively regulate the release profiles of the microspheres. Based on the results illustrated in Fig. 2, it can be reached that the presently built chitosan microspheres are not suitable for a sustained and prolonged release of TGF-β1 due to their high release rates and severe initial burst.

3.4.2. *Release profiles of microsphere-embedded scaffolds*

The release patterns of TGF-β1 from different scaffolds with similar pore parameters are presented in Fig. 3. In the cases of chitosan-PCL scaffolds, less than 8% of TGF-β1 was released in the first day, and afterwards, their release patterns followed approximately linear behavior longer than four weeks at various release rates. On the other hand, chitosan scaffolds showed typical burst release and most of TGF-β1 was released from these scaffolds within two weeks. In comparison with the cases of chitosan microspheres shown in Fig. 2, chitosan scaffolds still had the same characteristics of fast release and initial burst even though the release of TGF-β1 from chitosan scaffolds was relatively delayed. In addition, release rates of chitosan scaffolds were not significantly influenced by embedded microspheres. In contrast to this observations, the initial burst from chitosan-PCL scaffolds was greatly reduced, and the corresponding release rates were clearly down-regulated by the microspheres crosslinked with increasing amounts of crosslinker ($p < 0.05$). The SEM image shown in Fig. 1(B) demonstrated that the chitosan microspheres were coated to a certain extent by some chitosan-PCLs during the fabrication of scaffolds. It is known that PCL is highly hydrophobic and has a very low degradation rate under physiological conditions (Shalaby, 1994), and thus, the coating layer formed by chitosan-PCLs would retard the release of TGF-β1 because chitosan-PCLs had around 42 wt.% of PCL component which can partially prevent water from penetrating into microspheres and also resist the erosion from lysozyme. With respect to chitosan scaffolds, the coating effect of chitosan molecules on the microspheres might not be great enough because of the high sensitivity to lysozyme and hydrophilic characteristics of chitosan, leading to their similar release patterns as compared to the chitosan microspheres.

Fig. 4 presents the release behavior of TGF-β1 from chitosan-PCL scaffolds with different pore parameters. Like other chitosan-PCL

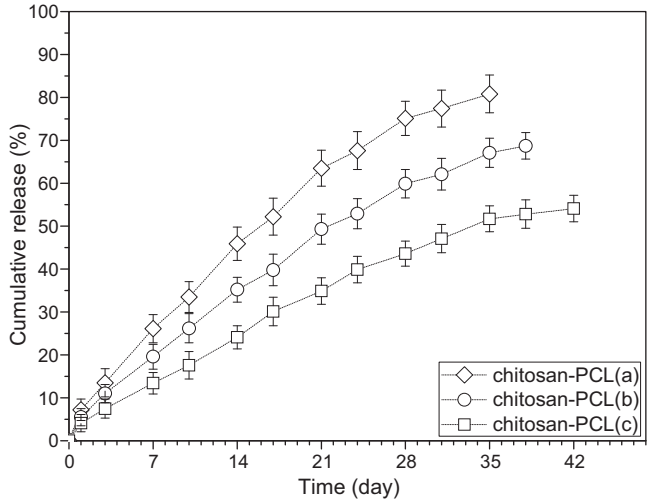

Fig. 4. Release profiles of microsphere-embedded scaffolds with different pore parameters.

scaffolds illustrated in Fig. 3, chitosan-PCL(a), chitosan-PCL(b) and CH-PCL(c) scaffolds showed low initial release of TGF-β1 and their release patterns also followed approximately linear characteristics for a period longer than four weeks. In addition, the plots in Fig. 4 indicate that pore parameters of the scaffolds can significantly modulate the release rates of the scaffolds ($p < 0.01$) and the scaffolds with higher porosity and larger average pore-size would have a higher release rate.

3.5. Kinetics of TGF-β1 release from microsphere-embedded scaffolds

Many different bioactive drugs have been delivered by using various polymer vehicles so far. Despite the diversity and complexity of various release systems some empirical models have been established to describe kinetics of release (Kumar, Muzzarelli, Muzzarelli, Sashiwa & Domb, 2004). In the case of swellable polymer matrices, the kinetic behavior of drug release can be estimated using following empirical equation (Yu and Xiao, 2008):

$$\frac{M_t}{M_\infty} = kt^n \quad \text{or} \quad \log\left(\frac{M_t}{M_\infty}\right) = \log k + n\log t \tag{4}$$

where M_t/M_∞ is the amount of released drug (%) at time t (d), k ($\%/d^n$) is a constant incorporating structural and geometric characteristics of drug-loaded devices as well as the release rate, and n is the release exponent, indicative of the mechanism of drug release. Based on the linear regression method, n and k can be calculated from the plots of log (M_t/M_∞) versus log t. Kinetic parameters for different chitosan-PCL scaffolds listed in Tables 2 and 3 are summarized in Table 4.

In the cases of slab or film systems, several specific values for n in Eq. (4) have distinct meanings. $n = 0.5$, drug-release follows a diffusion-controlled mechanism which is commonly regarded as Higuchi model; and $n = 1.0$, the rate of drug-release would be independent of time and this case is usually known as case-II transport or zero-order release kinetics. Values of n changed between 0.5 and 1.0 can be regarded as superposition of two apparently independent mechanisms, a Fickian diffusion and a case-II transport, and this kind of mechanism is commonly referred to as anomalous transport. In the case of a spherical carrier, the threshold of n-value differentiating between Fickian and non-Fickian diffusion is around 0.43, and n-values changed between 0.43 and 0.85 can be associated with anomalous transport.

Table 4
Estimated kinetic parameters of different chitosan-PCL scaffolds.

Sample[a]	k ($\%/d^n$)	n	r^2
Chitosan-PCL(I)	5.9	0.74	0.9937
Chitosan-PCL(II)	5.4	0.73	0.9959
Chitosan-PCL(III)	4.9	0.72	0.9908
Chitosan-PCL(IV)	3.9	0.72	0.9914
Chitosan-PCL(a)	6.7	0.72	0.9956
Chitosan-PCL(b)	5.1	0.72	0.9971
Chitosan-PCL(c)	3.6	0.73	0.9925

[a] See Tables 2 and 3 for the definition of sample names.

In the present cases, data in Table 4 indicate that n-values of scaffolds were slightly higher than 0.7 with correlation coefficients higher than 0.99, suggesting that release of TGF-β1 from these chitosan-PCL scaffolds is involved in an anomalous transport related to Fickian diffusion and case-II transport. It is also observed from Table 4 that the pore parameters exerted significant impacts on k-values of scaffolds while the embedded microspheres only slightly regulated the release rates of the scaffolds.

On the basis of above examinations, it can be reached that presently fabricated microsphere- embedded chitosan-PCL scaffolds are able to maintain required strength in wet state and also function as desirable carriers for the sustained and controlled release of TGF-β1 without severe initial burst over an extended period, suggesting their potential applications in articular cartilage repair.

4. Conclusions

The present study supports the sustained delivery of transforming growth factor-β1 using microsphere-embedded chitosan-polycaprolactone scaffolds as carriers. Some selected scaffolds built by chitosan-polycaprolactone with a proper weight percentage of polycaprolactone could administrate the release of transforming growth factor-β1 in an approximately linear manner longer than four weeks without severe initial burst. The release patterns of transforming growth factor-β1 from the scaffolds were governed by an anomalous transport mechanism, and the release rates of the scaffolds could be effectively regulated by the pore parameters of the scaffolds instead of the embedded microspheres. In addition, the presently fabricated chitosan-polycaprolactone scaffolds also showed desirable compressive properties in the wet state, suggesting that these scaffolds would be useful for the applications in articular cartilage repair where the local presence of transforming growth factor-β1 at a therapeutic level and the maintenance of required compressive strength of the scaffolds may be concurrently required.

Acknowledgement

The financial support for this work was provided by the National Natural Science Foundation of China (grant No. 81071470).

References

Chiang, H., & Jiang, C. C. (2009). Repair of articular cartilage defects: Review and perspectives. *Journal of the Formosan Medical Association*, *108*, 87–101.
Chung, C., & Burdick, J. A. (2008). Engineering cartilage tissue. *Advanced Drug Delivery Reviews*, *60*, 243–362.
Giannoni, P., & Hunziker, E. B. (2003). Release kinetics of transforming growth factor-β1 from fibrin clots. *Biotechnology and Bioengineering*, *83*, 121–123.
Haleem, M., & Chu, C. R. (2010). Advances in tissue engineering techniques for articular cartilage repair. *Operative Techniques in Orthopaedics*, *20*, 76–89.
Hoshiba, T., Jiang, H. L., Choi, Y. J., Akaike, T., Cho, C. S., Kim, B. S., & Park, I. K. (2011). Design of artificial extracellular matrices for tissue engineering. *Progress in Polymer Science*, *36*, 238–268.
Hunziker, E. B. (2001). Growth-factor-induced healing of partial-thickness defects in adult articular cartilage. *Osteoarthritis and Cartilage*, *9*, 22–32.

Hutmacher, D. W. (2000). Scaffolds in tissue engineering bone and cartilage. *Biomaterials*, *21*, 2529–2543.

Kumar, M. N. V. R., Muzzarelli, R. A. A., Muzzarelli, C., Sashiwa, H., & Domb, A. J. (2004). Chitosan chemistry and pharmaceutical perspectives. *Chemical Reviews*, *104*, 6017–6084.

Liu, L., Chen, L., & Fang, Y. (2006). Self-catalysis of phthaloylchitosan for graft copolymerization of ε-caprolactone with chitosan. *Macromolecular Rapid Communications*, *27*, 1988–1994.

Muzzarelli, R. A. A. (2009a). Chitins and chitosans for the repair of wounded skin, nerve, cartilage and bone. *Carbohydrate Polymers*, *76*, 167–182.

Muzzarelli, R. A. A. (2009b). Genipin-crosslinked chitosan hydrogels as biomedical and pharmaceutical aids. *Carbohydrate Polymers*, *77*, 1–9.

Muzzarelli, R. A. A. (2011). Chitosan composites with inorganics, morphogenetic proteins and stem cells, for bone regeneration. *Carbohydrate Polymers*, *83*, 1433–1445.

Ozbas-Turan, S., Akbuga, J., & Aral, C. (2002). Controlled release of interleukin-2 from chitosan microsphere. *Journal of Pharmaceutical Sciences*, *91*, 1245–1251.

Pearle, A. D., Warren, R. F., & Rodeo, S. A. (2005). Basic science of articular cartilage and osteoarthritis. *Clinics in Sports Medicine*, *24*, 1–12.

Puppi, D., Chiellini, F., Piras, A. M., & Chiellini, E. (2010). Polymeric materials for bone and cartilage repair. *Progress in Polymer Science*, *35*, 403–440.

Qu, X., Wirsen, A., & Albertsson, A. C. (1999). Synthesis and characterization of pH-sensitive hydrogels based on chitosan and D,L-lactic acid. *Journal of Applied Polymer Science*, *74*, 3193–3202.

Rutgersy, M., Pelty, M. J. P. V., Dhertyz, W. J. A., Creemersy, L. B., & Saris, D. B. F. (2010). Evaluation of histological scoring systems for tissue-engineered, repaired and osteoarthritic cartilage. *Osteoarthritis and Cartilage*, *18*, 12–23.

Shalaby, S. W. (1994). *Biomedical polymers*. New York: Hanser Publishers.

Sterodimas, A., Faria, J. D., Correa, W. E., & Pitanguy, I. (2009). Tissue engineering and auricular reconstruction: A review. *Journal of Plastic Reconstructive and Aesthetic Surgery*, *62*, 447–452.

Whitaker, M. J., Quirk, R. A., Howdle, S. M., & Shakesheff, K. M. (2001). Growth factor release from tissue engineering scaffolds. *Journal of Pharmacy and Pharmacology*, *53*, 1427–1437.

Wan, Y., Creber, K. A. M., Peppley, B., & Bui, V. T. (2003). Synthesis, characterization and ionic conductive properties of phosphorylated chitosan membranes. *Macromolecular Chemistry and Physics*, *204*, 850–858.

Wu, H., Zhang, J., Xiao, B., Zan, X., Gao, J., & Wan, Y. (2011). *N*-(2-hydroxypropyl)-3-trimethylammonium chitosan-poly(ε-caprolactone) copolymers and their antibacterial activity. *Carbohydrate Polymers*, *83*, 824–830.

Wan, Y., Wu, H., Xiao, B., Cao, X., & Dalai, S. (2009). Chitosan-g-polycaprolactone copolymer fibrous mesh scaffolds and their related properties. *Polymers for Advanced Technologies*, *20*, 795–801.

Yu, H. Q., & Xiao, C. B. (2008). Synthesis and properties of novel hydrogels from oxidized konjac glucomannan crosslinked gelatin for in vitro drug delivery. *Carbohydrate Polymers*, *72*, 479–489.

Yuan, Y., Chesnutt, B. M., Utturkar, G., Haggard, W. O., Yang, Y., Ong, J. L., & Bumgardner, J. D. (2007). The effect of cross-linking of chitosan microspheres with genipin on protein release. *Carbohydrate Polymers*, *68*, 561–567.